Gold Catalysis

DOI: 10.1002/anie.201101612

Low-Temperature Catalytic H_2 Oxidation over Au Nanoparticle/TiO_2 Dual Perimeter Sites**

*Isabel Xiaoye Green, Wenjie Tang, Matthew Neurock, and John T. Yates Jr.**

Dedicated to Professor Gerhard Ertl on the occasion of his 75th birthday and to the Fritz Haber Institute, Berlin, on the occasion of its 100th anniversary

The catalytic oxidation of H_2 is of great interest due to its role in H_2O_2 synthesis, catalytic oxidation of hydrocarbons, and the selective removal of CO from hydrogen streams[1] as well as for its simplicity which makes it ideal for fundamental bond making and breaking studies. This is especially true for supported Au nanoparticles which were found to show unusually high activity by Haruta et al.[2] Previous explanations for this activity have invoked quantum size effects for Au particles in the 2 nm range,[3] electronic effects in thin films of Au,[4] and enhancement of the fraction of perimeter sites.[5] Recent experiments on inverse TiO_2/Au catalysts have suggested that the enhanced catalytic activity may be due to active sites at the TiO_2/Au interface rather than a quantum size effect.[5b,6]

The presence of H_2 gas in CO + O_2 reaction streams is known to produce enhanced catalytic activity for CO oxidation over Au/TiO_2 catalysts. The promotional effect originates from the addition of H_2 and has been ascribed to H_2's ability to regenerate the catalyst by reducing the hydrocarbon accumulation[1d,e] or by its reaction with O_2 to form hydroperoxy (OOH*) intermediates which readily oxidize CO.[7] Previous theoretical studies have provided unique insights for this reaction, but have only focused on the role of Au.[7c,8] To our best knowledge, there are no reported theoretical studies on the H_2 + O_2 reaction that have considered the influence or involvement of the TiO_2 perimeter sites at the Au–TiO_2 interface. Herein, we use kinetic analyses together with in situ infrared spectroscopic studies and density functional theory (DFT) calculations to examine the activity of the Au sites as well as the Au and TiO_2 perimeter sites at the Au–TiO_2 interface and elucidate a plausible reaction mechanism. (We define a perimeter site as a Au or TiO_2 site at the external boundary between Au and TiO_2 surfaces. A dual perimeter site involves a Au perimeter site and a TiO_2 perimeter site that operate together during the catalytic reaction.)

High-vacuum transmission IR experiments were used to follow H_2O production on Au/TiO_2 powder synthesized by the deposition–precipitation method (see Supporting Information, sections I, II and Figure S1 for further details).[9] The average Au particle size is approximately 3 nm, determined by transmission electron microscopy (Figure S2).

It has been reported that atomic H dissolved in TiO_2[10] may be detected by the IR background upward shift, which is caused by trapped electrons from H in the conduction band

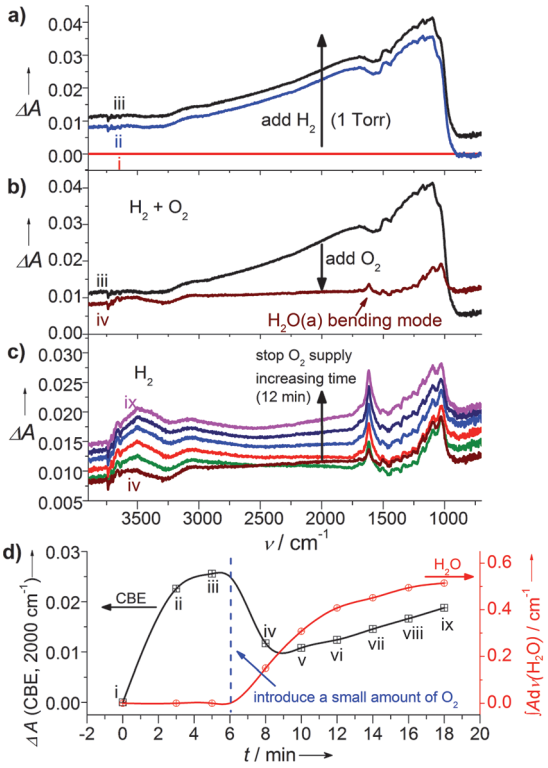

Figure 1. a) IR difference spectra of the H_2 spillover and CBE background shifting effect on the Au/TiO_2 at 295 K under 1 Torr of H_2. b) IR difference spectra of the H_2 oxidation by O_2 over the Au/TiO_2 at 295 K. c) IR difference spectra of the CBE background shifting effect on the (partially H_2O-covered) Au/TiO_2 surface when the O_2 supply is cut off. d) Plot of the CBE (left) and H_2O (right) development against time during the above processes.

[*] I. X. Green, Prof. Dr. M. Neurock, Prof. Dr. J. T. Yates Jr.
Department of Chemistry, University of Virginia
Charlottesville, VA 22904 (USA)
Fax: (+1) 434-243-8695
E-mail: jty2n@virginia.edu
Dr. W. Tang, Prof. Dr. M. Neurock
Department of Chemical Engineering, University of Virginia
Charlottesville, VA 22904 (USA)

[**] We gratefully acknowledge the support of this work by the U.S. Department of Energy-Office of Basic Energy Sciences (DE-FG02-09ER16080), the National Science Foundation, and the Texas Advanced Computing Center for Teragrid resources. We also acknowledge the helpful discussion with Dr. Zhen Zhang of the University of Virginia.

Supporting information for this article is available on the WWW under http://dx.doi.org/10.1002/anie.201101612.

edge (CBE) states (Figure S3).[11] Examples of this phenomenon at room temperature are shown in Figure 1a and S4, where a substantial IR background up-shift is caused by molecular H_2 dissociation on Au followed by atomic H spillover to the TiO_2 support. Figure 1b shows that when a small quantity of O_2 is introduced to the H-rich surface, it drains the CBE electrons which results in an immediate background drop. Simultaneously, the oxidation reaction of the H_2 on the Au/TiO_2 surface to form H_2O(a) is observed by the absorption band at 1620 cm^{-1} (δ_{H_2O}).[1d,12] Removal of O_2 by reaction causes the CBE to return to an increased level in the H_2-rich environment (Figure 1c). The whole process is summarized in Figure 1d where both the CBE change and the H_2O formation are plotted with respect to time.

In an effort to observe more details of the H_2–O_2 reaction, the catalyst was cooled to 210 K and a 1:100 mixture of O_2 and H_2 was added. The reaction progress is shown in Figure 2,

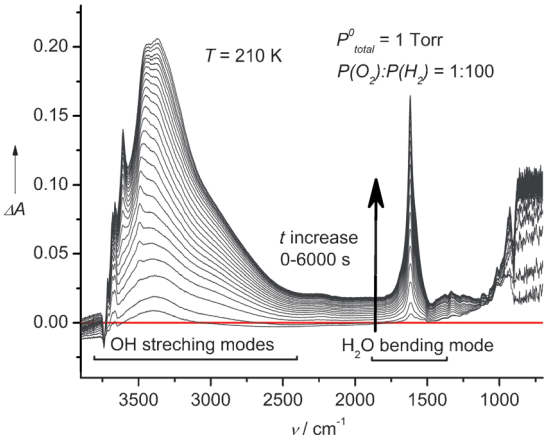

Figure 2. IR difference spectra of the Au/TiO_2 surface during H_2 oxidation by O_2 at 210 K.

indicating the production of both H_2O(a) and OH. A search for peroxide intermediate within the 1505–900 cm^{-1} region was inconclusive.[13] No products were observed on a pure TiO_2 sample mounted below the catalyst for the same reaction conditions (Figure S1), indicating that Au is necessary for the reaction. Similar experiments over the temperature range of 200–220 K were carried out and the kinetics studies as a function of temperature are shown in Figure 3. An Arrhenius plot of the initial rate is shown in the inset, yielding an apparent activation energy of 0.22 ± 0.02 eV. This is the first report of the kinetics of H_2 oxidation over Au/TiO_2 below room temperature. Activation energies at temperatures above 300 K have been measured as 0.38 eV for $H_2 + O_2$[14] and 0.37 eV for H_2–D_2 exchange.[5b] The rate of reaction maximizes to nearly the same limit at particular pressures of O_2 (ca. 0.08 Torr) and H_2 (ca. 1.4 Torr), as shown in Figure 4, indicating site saturation for both reactants.

DFT calculations were carried out to help elucidate the reaction mechanism and identify possible active sites for the low temperature H_2 oxidation (Supporting Information, Section III). The Au structure on the rutile TiO_2(110) surface was simulated with a Au nanorod covalently bound to the

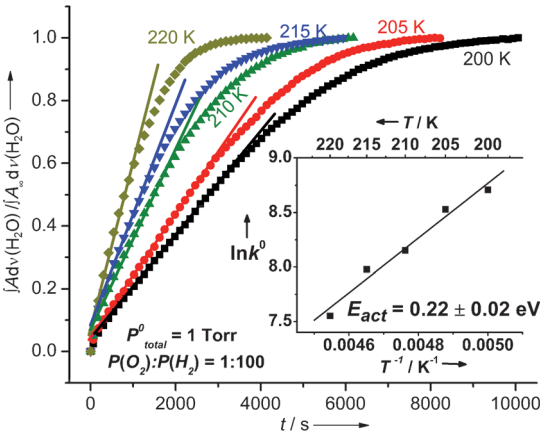

Figure 3. Kinetics for the oxidation of H_2 by O_2 over the Au/TiO_2 catalyst as measured by the change in the absorbance of H_2O as a function of time and temperature. The inset shows the Arrhenius plot.

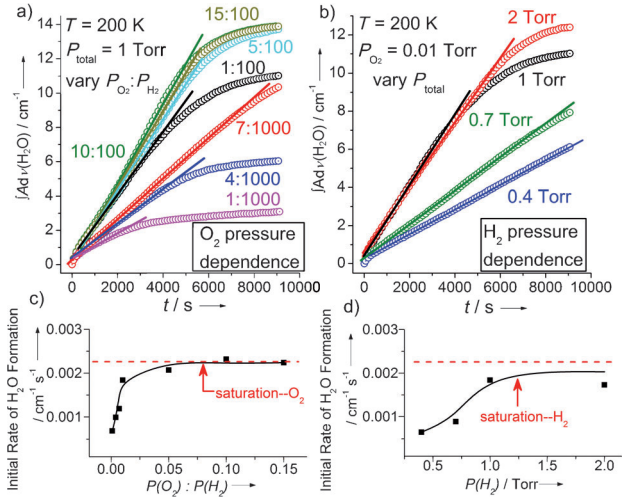

Figure 4. The effects of: a) O_2 pressure and b) H_2 pressure on the H_2 oxidation kinetics over Au/TiO_2. c) Plot of the initial rate of H_2O formation as a function of increasing O_2 partial pressure. d) Plot of the initial rate of H_2O formation as a function of the increasing H_2 pressure.

surface as shown in Figure S5. This configuration was used previously[15] as it provides a distribution of different Au sites in contact with the support. Although not identical to the experimentally used catalyst, it is believed that the fundamental steps modeled in our simplified simulations provide viable insights. H_2 oxidation is thought to proceed by the formation of two H adatoms. Our DFT results as well as previous experiments[11a] show that the lowest H–H dissociation barrier on Au in the absence of O_2 is approximately 0.5 eV (Figure S6). The calculations indicate that the local presence of adsorbed O_2 can promote H_2 dissociation to yield the activation energy of 0.22 eV measured experimentally.

The adsorption of O_2 at the Ti_{5c} perimeter site, the most favored of all of the sites shown in Figure S7, indeed, lowers the barrier for the dissociative adsorption of H_2(g) at the neighboring Au perimeter site down to 0.16 eV, as shown in Figure 5a,b. The dissociative adsorption of H_2 at this dual

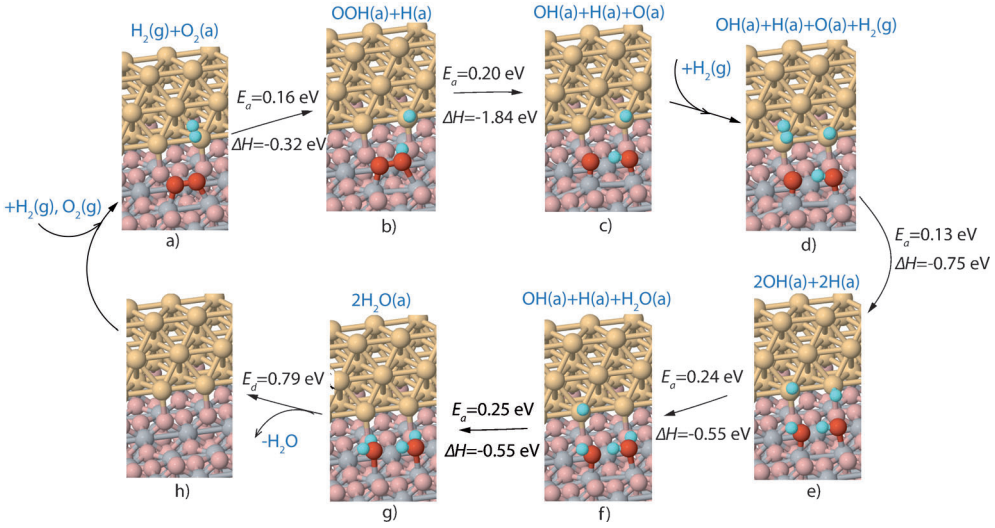

Figure 5. Catalytic reaction cycle and the corresponding activation barriers for the individual steps of the mechanism for the oxidation of H_2 to form H_2O over model Au/TiO_2 structures. The Au atoms and Ti atoms are shown in yellow and grey, respectively, whereas the O in the TiO_2 lattice, adsorbed O, and H atoms are shown in pink, red, and cyan, respectively. E_a and ΔH represent activation barriers and reaction energies separately.

perimeter site thus produces Ti–OOH intermediate and Au–H surface intermediates. Dissociation of the Ti–OOH to form Ti–OH and Ti–O was calculated to have a barrier of 0.20 eV (Figure 5c). The resulting O(a) activates and dissociates a second incident H_2(g) at the dual perimeter site, with a barrier of 0.13 eV, as shown in Figure 5e. The final hydrogenation of the two Ti–OH species by the two Au–H species proceeds with activation energies of 0.24 and 0.25 eV, as shown in Figure 5 f,g.

The initial rate of H_2O formation involves a sequence of elementary steps (Figure 5a–g) that have rather low activation energies in the range 0.13–0.25 eV. While it is difficult to rigorously distinguish a rate-controlling step, the hydrogenation of OH(a) to form H_2O has the highest activation energy of 0.25 eV, in good agreement with the measured E_a of 0.22 eV. The low barriers of all other steps (Figure 5a–h) suggest that the Au/TiO_2 perimeter sites serve as active sites for the H_2 oxidation at low temperature, through an O_2-assisted H–H dissociation mechanism.

Calculations of H_2O surface diffusion energies on TiO_2 (estimated to be 0.21, 0.32, and 0.43 eV at 1, 2/3, and 1/3 monolayer (ML) coverages) and desorption energy (0.79 eV in Figure 5g,h) suggest that H_2O will cluster and accumulate to block the active perimeter sites at low temperatures as the reaction proceeds. This is consistent with the results presented in Figure 3 where the reaction stops at longer times. Our measurements have therefore focused on the initial reaction rates where the effect of site blockage is minimal. This also means that the kinetic studies shown in Figure 3 are controlled by the disappearance of the active sites for H_2 oxidation.

To further elucidate the mechanism, we carried out D_2 labeling studies to measure the kinetic isotope effect (KIE). The rates of reaction of O_2 with H_2 and D_2 at 200 K, which are compared in Figure 6, show a ca. 7-fold increase in the initial rates for H_2 over D_2. The zero point energy (ZPE) differences for the reactant H_2 and D_2 and the corresponding transition states (TS) were considered in order to calculate the KIE to compare with the experimental results. The inset of Figure 6 shows the calculated initial state and TS and the corresponding vibrational frequencies of the H_2 dissociation reaction (steps a and b in Figure 5). If the ZPE difference is taken only for the initial state, the rate ratio, k_H/k_D, is calculated to be 87. Instead, using both initial and transition state frequencies, the calculated $k_H/k_D = 5$, in good agreement with the experimentally measured KIE value of 7, and indicating that an early TS is involved.

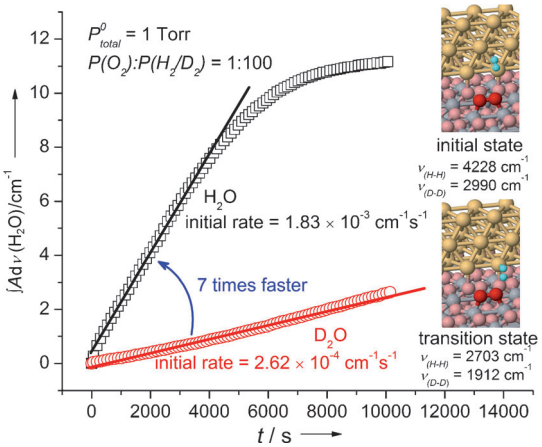

Figure 6. D_2 kinetic isotope effect for the oxidation of H_2 by O_2 over the Au/TiO_2 catalyst at 200 K. The insets show the ab initio calculated initial state and transition state frequencies for the O_2-assisted H_2 dissociation process.

In summary, the active site for the $H_2 + O_2$ reaction over a Au/TiO_2 nanoparticle catalyst at low temperature was located at dual perimeter sites at the interface between Au and TiO_2. An O_2-assisted H_2 dissociation through a Ti–OOH intermediate was proposed involving an early transition state. The calculated activation energies for sequential steps in the range 0.13–0.25 eV agree with the measured apparent activation energy of 0.22 eV.

Received: March 4, 2011
Published online: May 31, 2011

Keywords: gold catalysis · H_2 oxidation · kinetic isotope effect · perimeter site · titania support

[1] a) C. Song, *Catal. Today* **2002**, *77*, 17 – 49; b) G. C. Bond, D. T. Thompson, *Catal. Rev. Sci. Eng.* **1999**, *41*, 319 – 388; c) J. P. Collman, L. M. Slaughter, T. A. Eberspacher, T. Strassner, J. I. Brauman, *Inorg. Chem.* **2001**, *40*, 6272 – 6280; d) B. Schumacher, Y. Denkwitz, V. Plzak, M. Kinne, R. J. Behm, *J. Catal.* **2004**, *224*, 449 – 462; e) M. Azar, V. Caps, F. Morfin, J.-L. Rousset, A. Piednoir, J.-C. Bertolini, L. Piccolo, *J. Catal.* **2006**, *239*, 307 – 312.

[2] M. Haruta, T. Kobayashi, H. Sano, N. Yamada, *Chem. Lett.* **1987**, 405 – 408.

[3] M. Valden, X. Lai, D. W. Goodman, *Science* **1998**, *281*, 1647 – 1650.

[4] M. S. Chen, D. W. Goodman, *Science* **2004**, *306*, 252 – 255.

[5] a) M. Kotobuki, R. Leppelt, D. A. Hansgen, D. Widmann, R. J. Behm, *J. Catal.* **2009**, *264*, 67 – 76; b) T. Fujitani, I. Nakamura, T. Akita, M. Okumura, M. Haruta, *Angew. Chem.* **2009**, *121*, 9679 – 9682; *Angew. Chem. Int. Ed.* **2009**, *48*, 9515 – 9518; c) N. Lopez, T. V. W. Janssens, B. S. Clausen, Y. Xu, M. Mavrikakis, T. Bligaard, J. K. Nørskov, *J. Catal.* **2004**, *223*, 232 – 235; d) F. Cárdenas-Lizana, S. Gómez-Quero, H. Idriss, M. A. Keane, *J. Catal.* **2009**, *268*, 223 – 234.

[6] J. A. Rodriguez, S. Ma, P. Liu, J. Hrbek, J. Evans, M. Perez, *Science* **2007**, *318*, 1757 – 1760.

[7] a) L. Piccolo, H. Daly, A. Valcarcel, F. C. Meunier, *Appl. Catal. B* **2009**, *86*, 190 – 195; b) E. Quinet, L. Piccolo, F. Morfin, P. Avenier, F. Diehl, V. Caps, J.-L. Rousset, *J. Catal.* **2009**, *268*, 384 – 389; c) D. C. Ford, A. U. Nilekar, Y. Xu, M. Mavrikakis, *Surf. Sci.* **2010**, *604*, 1565 – 1575.

[8] a) D. G. Barton, S. G. Podkolzin, *J. Phys. Chem. B* **2005**, *109*, 2262 – 2274; b) A. M. Joshi, W. N. Delgass, K. T. Thomson, *J. Phys. Chem. B* **2005**, *109*, 22392 – 22406; c) F. Wang, D. Zhang, H. Sun, Y. Ding, *J. Phys. Chem. C* **2007**, *111*, 11590 – 11597; d) L. Barrio, P. Liu, J. A. Rodriguez, J. M. Campos-Martin, J. L. G. Fierro, *J. Phys. Chem. C* **2007**, *111*, 19001 – 19008.

[9] a) I. X. Green, J. T. Yates, Jr., *J. Phys. Chem. C* **2010**, *114*, 11924 – 11930; b) S. Kim, O. Byl, J. T. Yates, Jr., *J. Phys. Chem. B* **2005**, *109*, 3499 – 3506; c) R. Zanella, S. Giorgio, C. R. Henry, C. Louis, *J. Phys. Chem. B* **2002**, *106*, 7634 – 7642.

[10] a) X. L. Yin, M. Calatayud, H. Qiu, Y. Wang, A. Birkner, C. Minot, C. Wöll, *ChemPhysChem* **2008**, *9*, 253 – 256; b) G. H. Enevoldsen, H. P. Pinto, A. S. Foster, M. C. R. Jensen, W. A. Hofer, B. Hammer, J. V. Lauritsen, F. Besenbacher, *Phys. Rev. Lett.* **2009**, *102*, 136103; c) H. Noei, H. Qiu, Y. Wang, M. Muhler, C. Wöll, *ChemPhysChem* **2010**, *11*, 3604 – 3607.

[11] a) D. A. Panayotov, J. T. Yates, Jr., *J. Phys. Chem. C* **2007**, *111*, 2959 – 2964; b) D. A. Panayotov, J. T. Yates, Jr., *Chem. Phys. Lett.* **2005**, *410*, 11 – 17; c) D. A. Panayotov, J. T. Yates, Jr., *Chem. Phys. Lett.* **2007**, *436*, 204 – 208.

[12] X. Wang, S. Kim, C. Buda, M. Neurock, O. B. Koper, J. T. Yates, Jr., *J. Phys. Chem. C* **2009**, *113*, 2228 – 2234.

[13] C. Sivadinarayana, T. V. Choudhary, L. L. Daemen, J. Eckert, D. W. Goodman, *J. Am. Chem. Soc.* **2004**, *126*, 38 – 39.

[14] G. Walther, D. J. Mowbray, T. Jiang, G. Johnes, S. Jensen, U. J. Quaade, S. Horch, *J. Catal.* **2008**, *260*, 86 – 92.

[15] a) L. M. Molina, M. D. Rasmussen, B. Hammer, *J. Chem. Phys.* **2004**, *120*, 7673 – 7680; b) S. Laursen, S. Linic, *Phys. Chem. Chem. Phys.* **2009**, *11*, 11006 – 11012.

